Hindawi
Shock and Vibration
Volume 2018, Article ID 3845353, 9 pages
https://doi.org/10.1155/2018/3845353

Research Article

Experimental Study on Thermal Damage and Energy Evolution of Sandstone after High Temperature Treatment

Rong-rong Zhang[1,2] **Lai-wang Jing**[1,2] **and Qin-yong Ma**[1,2]

[1] *Engineering Research Center of Underground Mine Construction, Ministry of Education, Anhui University of Science and Technology, Huainan 232001, China*
[2] *School of Civil Engineering and Architecture, Anhui University of Science and Technology, Huainan 232001, China*

Correspondence should be addressed to Rong-rong Zhang; zrrah187@163.com

Received 8 February 2018; Accepted 27 March 2018; Published 27 June 2018

Academic Editor: Marco Alfano

Thermal damage and energy evolution characteristics in process of impact failure of sandstone after high temperature treatment were studied by split Hopkinson pressure bar (SHPB) system. The ultrasonic P-wave velocity, density, porosity, peak stress, E_T/E_0, thermal damage, fracture, and energy evolution characteristics of sandstone with temperature during the experimental process were explored. Results show that, with the increase of temperature, the ultrasonic P-wave velocity and density decrease, while the porosity increases. It is found that the peak stress and E_T/E_0 decrease with the increase of temperature, and the decreasing trend is fitted with the simple cubic equation. Above 600°C, dynamic peak stress and E_T/E_0 decrease rapidly. The thermal damage of rock increases with the increase of temperature, which is in accordance with the logistic curve model. The thresholds of damage strain energy release rate are 200°C and 800°C in this research. Its total input strain energy decreases with the increase of processing temperature and decreases sharply when the temperature is over 600°C. The variation of total input strain energy has small change at the range from 400°C to 600°C.

1. Introduction

Underground mining and utilization of deep underground space have long been considered a high-risk activity. So far, many studies have been related to deep mining of hard rock mines and utilization [1, 2]. The study of physical and mechanical properties, impact damage, and energy dissipation of rocks after high temperature has aroused great concern. Meanwhile, a series of difficult problems have been put forward for the mining of deep rocks and the utilization of deep underground space [3, 4].

Deep mining and utilization are related to the dynamic properties of rocks under different temperature environments [5]. To study the dynamic damage and energy dissipation of sandstone after high temperature treatment, many experts and scholars have carried out a series of experiments and obtained the experimental results. Zhang et al. [6] measured the dynamic fracture toughness of Fangshan gabbro and Fangshan marble subjected to high temperature by split Hopkinson pressure bar (SHPB) system. Liu and Xu [7, 8] carried out the dynamic mechanical experiments on marble under different temperature and different strain rates by using the high temperature split Hopkinson pressure bar (SHPB) experimental system. There are linear relationships among peak stress, peak strain, and elastic modulus with the temperature. Yin et al. [9, 10] analyzed the stress-strain curve, elastic modulus, dynamic damage, and energy dissipation of rock. Kong et al. [11] studied the differences in the thermal mechanical properties and acoustic emission (AE) characteristics during the deformation and fracture of rock under the action of continuous heating and after high temperature treatment. Zhou et al. [12] proposed an inversion model of rock damage based on microseismic moment tensor. A numerical simulation of rock mass damage that couples joints, water, and microseismicity was performed. The rock mass damage mechanism was then analyzed. Li and Gu [13] analyzed the difference in the rock's energy dissipation under different loading waveforms and explored the theory of rock's

energy dissipation under different loading waves. Jin et al. [14] found that the incident energy, strain energy, and dissipation energy of a specimen show approximate increasing trends as the flaw angle increases.

Rocks are composed by mineral particles with various chemical compositions and different degrees of crystallization. The internal structure of rock is complex and its dispersion is large. In this article, the dynamic failure characteristics of sandstone after high temperature treatment were studied by using a split Hopkinson pressure bar (SHPB) system. The ultrasonic P-wave velocity, the evolution of thermal damage, the failure mode, and the energy dissipation of the specimen are analyzed to characterize the dynamic features of the sandstone. The effect of temperature on the physical and mechanical properties of rock is analyzed.

2. Specimen Preparation and Experiment Setup

2.1. Sample Preparation. The fine-grained sandstone was −906 m level and collected in the Zhujidong coalmine located in Huainan city, Anhui province, China. The main components of sandstone are quartz, feldspar, and dolomite [15–17]. Rock samples were processed into cylindrical specimens of 50 mm × 25 mm by cutting and polishing. Both planes of each specimen were ground to ensure that both planes were parallel with accuracy of ±0.05 mm and both planes were perpendicular to the longitudinal axis with accuracy of ±0.25° (ISRM) [18].

Before the test, all samples were numbered and grouped according to different temperature levels. The temperature scope on deep sandstone ranges from 20°C to 1000°C and the impact loading pressure is 0.85 MPa and 1.05 MPa, respectively. Test was divided into six temperature grades: 20°C (room temperature), 200°C, 400°C, 600°C, 800°C, and 1000°C, and each group was equipped with no less than 6 specimens.

2.2. Thermal and Testing Equipment. The heating device is a SX-5-12 box-type resistance furnace, which is composed of the control box and the furnace. The resistance furnace can heat the specimens to a maximum temperature of 1200°C. Sandstone specimens were heated in a resistance furnace at a rate of 6°C/min till the desired temperature. The desired temperature is kept constant for 4 h. After that, the specimens are left in the furnace to cool down to room temperature. The mass, volume, and P-wave velocity of these samples were tested before and after heating.

The dynamic impact loading test of sandstone was carried out by the SHPB system with a diameter of 50 mm which belongs to Anhui University of Science and Technology.

3. Experimental Data and Analysis

3.1. Variation in Ultrasonic P-Wave Velocity. Under natural state, the velocity of ultrasonic P-wave is a comprehensive embodiment of the elastic coefficients, deformation characteristics, and damage degree of rock material [19, 20]. The ultrasonic P-wave velocity of sandstone measured before and after high temperature treatment is shown in Figure 1. Before heat treatment, the average wave velocities of the specimens ranged from 3400 m/s to 3440 m/s. However, for specimens after heat treatment, it shows overall decrease of velocity; among those from 20°C to 200°C, the drop rate was relatively slow.

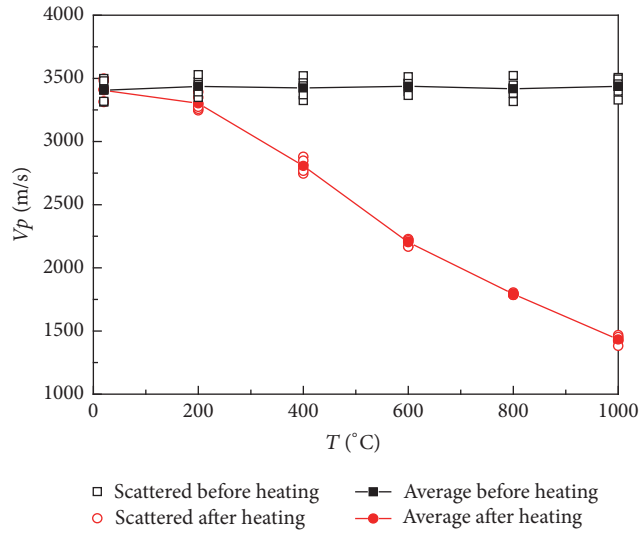

Figure 1: Relation of ultrasonic P-wave velocity before and after temperature treatment.

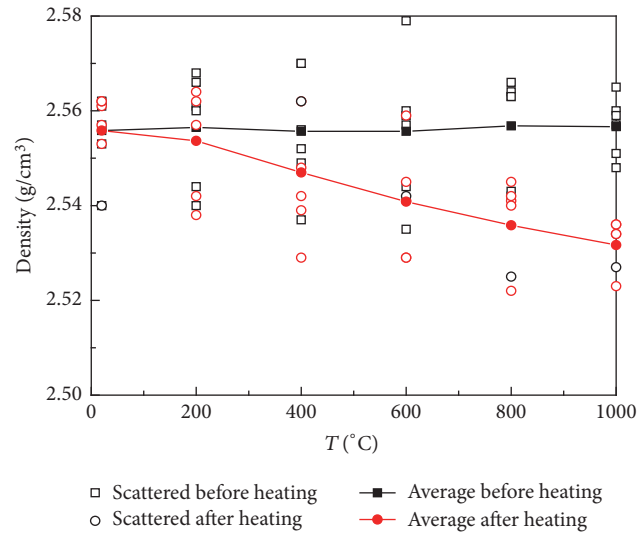

Figure 2: Variation of density versus temperature of sandstone.

The reason for decrease of ultrasonic P-wave velocity is explained as follows. On the one hand, the different states of water inside the rock will form water vapor and escape from the cracks under high temperature conditions, which aggravate the formation and expansion of the cracks and pores. On the other hand, the differences among the thermal expansion coefficients of the internal mineral components of rock and the strain between crystal and fissure lead to flaw and exfoliation of rock after high temperature treatment.

3.2. Variation in Density and Porosity. The variation of density and porosity before and after heating is shown in Figures 2 and 3. Below 200°C, the density drops slowly relatively. After

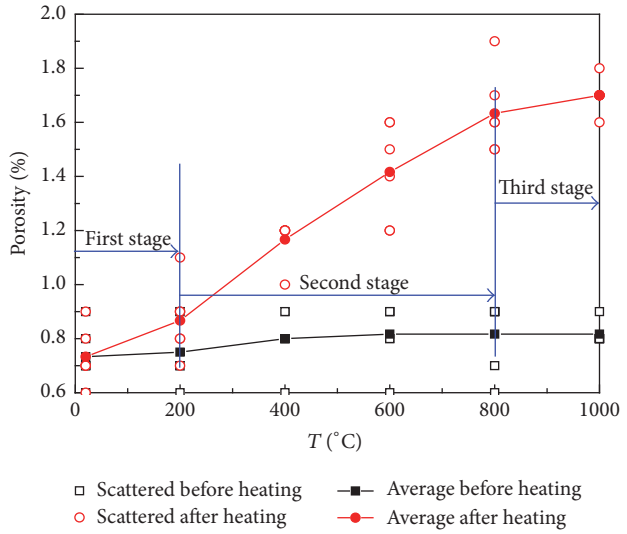

FIGURE 3: Variation of porosity versus temperature of sandstone.

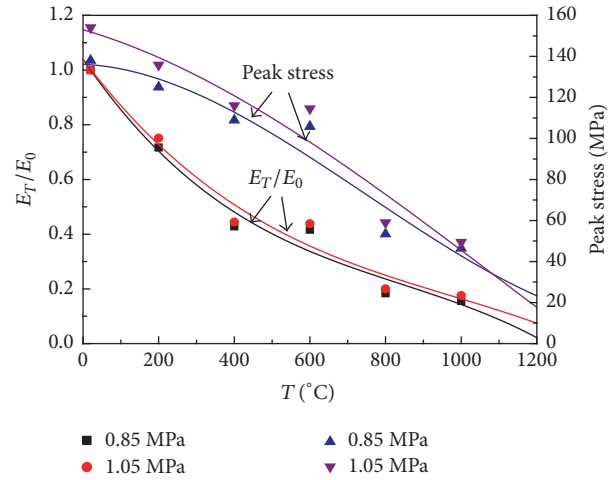

FIGURE 4: Relation of peak stress and E_T/E_0 with temperature.

that, it drops obviously. Because of deformation changes in structure lead to expansion and fine surface grains on the samples may flack under temperature deformation [8].

Figure 3 shows the evolution curve between porosity of sandstone samples and temperature. The evolution can be divided into three different stages. The different states of water (attached water, bound water, and mineral combined water) that exist inside the rock will evaporate after high temperature treatment [21]. In the first phase, from 20°C to 200°C, the porosity average increases from 0.73% to 0.87% slowly, and the increase rate is 18.28%. The stage is mainly due to the increase of porosity caused by evaporation of water in the rock. In the second phase, from 200°C to 800°C, the porosity average increases from 0.87% to 1.63% rapidly, and the increase rate is 88.35%. With the increase of temperature, the internal mineral water evaporates continuously, which leads to the increasing of mineral composition and microcracks in the rock. On the one hand, the change of microcracks increases the porosity. On the other hand, it destroys the original small network structure and greatly improves the connectivity of osmotic system and improves the capacity of channel flow. In the third phase, from 800°C to 1000°C, the porosity average increases slowly from 1.63% to 1.70%, and the corresponding to the increase rate is 4.10%. There seems to be a threshold at about 800°C and beyond which porosity average increase does not change a little.

3.3. Variation in Peak Stress and Relative Elastic Modulus (E_T/E_0). Variation in peak stress and relative elastic modulus with temperature is shown in Figure 4. With the increase of temperature, the peak stress and relative elastic modulus show a trend of gradual reduction. For sandstone, when the temperature exceeds a certain range, obvious deterioration will occur. From 20°C (room temperature) to 200°C, dynamic peak stress decreases by 9.45% and 11.81% at 0.85 Mpa and 1.05 Mpa. From 200°C to 400°C, dynamic peak stress decreases by 12.88% and 14.59% at 0.85 Mpa and 1.05 Mpa. Between 400°C and 600°C, dynamic peak stress is almost unchanged. Above 600°C, dynamic peak stress decreases rapidly. By regression analysis, peak stress and temperature meet the following equation:

0.85 MPa:

$$\sigma = 136.128 - 0.767\left(\frac{T}{100}\right) - 1.542\left(\frac{T}{100}\right)^2 + 0.068\left(\frac{T}{100}\right)^3 \quad R^2 = 0.845. \tag{1}$$

1.05 MPa:

$$\sigma = 152.983 - 5.311\left(\frac{T}{100}\right) - 0.776\left(\frac{T}{100}\right)^2 + 0.023\left(\frac{T}{100}\right)^3 \quad R^2 = 0.854. \tag{2}$$

E_T is the dynamic elastic modulus of rock treated with corresponding temperature and E_0 is the dynamic elastic modulus of rock at 20°C (room temperature) in Figure 4. The variation regularity is the same as the peak stress, which accords with the following fitting formula.

0.85 MPa:

$$\frac{E_T}{E_0} = 1.040 - 2.030\left(\frac{T}{1000}\right) + 1.868\left(\frac{T}{1000}\right)^2 - 0.739\left(\frac{T}{1000}\right)^3 \quad R^2 = 0.942. \tag{3}$$

1.05 MPa:

$$\frac{E_T}{E_0} = 1.039 - 1.830\left(\frac{T}{1000}\right) + 1.448\left(\frac{T}{1000}\right)^2 - 0.496\left(\frac{T}{1000}\right)^3 \quad R^2 = 0.932. \tag{4}$$

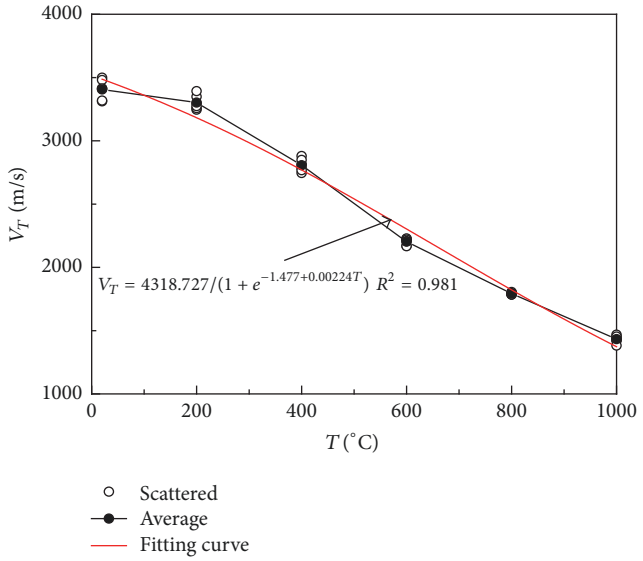

Figure 5: Relation of ultrasonic P-wave velocity after high temperature treatment with temperature.

3.4. Variation in Thermal Damage. Because of the different deformation of various mineral crystals in the rock, when the temperature changes, there will be a stress field inside the rock, which will promote the evolution and expansion of the microcracks and lead to the deterioration of the rock properties. As a result, the ultrasonic P-wave velocity will decrease to a certain extent. Relation of ultrasonic P-wave velocity after high temperature treatment with temperature is shown in Figure 5. The fitting formulas of the curve can be, respectively, obtained as follows:

$$V_T = \frac{4318.727}{\left(1 + e^{-1.477+0.00224T}\right)} \quad R^2 = 0.981. \tag{5}$$

In this test, damage is according to ultrasonic P-wave velocity:

$$D = 1 - \left(\frac{V_T}{V_0}\right)^2, \tag{6}$$

where D stands for thermal damage, V_T is ultrasonic P-wave velocity at temperature T, and V_0 is ultrasonic P-wave velocity at room temperature.

It can be seen from Figure 6 that the thermal damage of sandstone increases with the increase of temperature. The trend of porosity with temperature is basically the same. The fitting formulas of thermal damage and porosity of sandstone after high temperature treatment are obtained as follows:

$$\begin{aligned} D &= \frac{0.817}{\left(1 + e^{3.508-0.0075T}\right)} \quad R^2 = 0.991 \\ \gamma &= \frac{1.974}{\left(1 + e^{0.661-0.0026T}\right)} \quad R^2 = 0.986, \end{aligned} \tag{7}$$

where γ is porosity of sandstone.

The fitting curve of thermal damage of rock treated by temperature is simplified to thermal damage model (8),

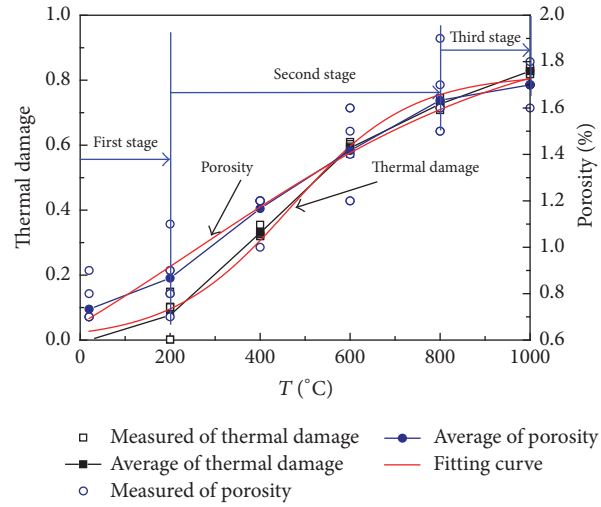

Figure 6: Relation of thermal damage and porosity with temperature.

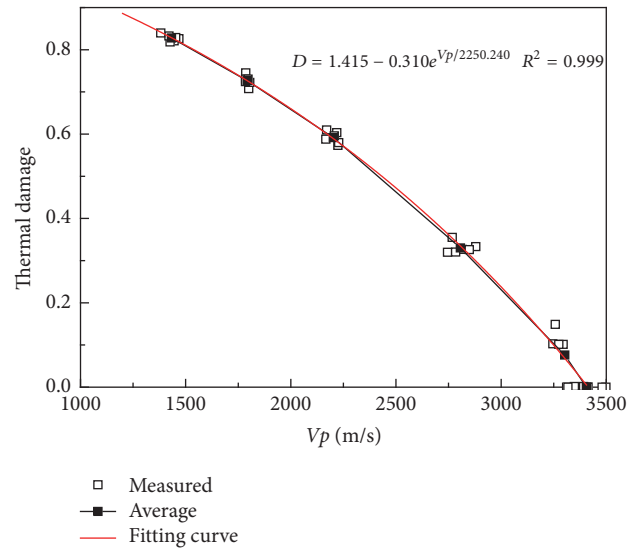

Figure 7: Relation of thermal damage and ultrasonic P-wave velocity.

which accords with logistic curve model [22]. It is seen that the logistic model can well reflect the nonlinearity of thermal damage evolution of sandstone exposed to different treatment temperatures.

$$D = \frac{\alpha}{\left(1 + e^{\beta - \eta T}\right)}, \tag{8}$$

where α, β, and η are constants.

Figures 7 and 8 show the relationship among wave velocity, porosity, and thermal damage. With the increase of ultrasonic P-wave velocity, the thermal damage decreases and the thermal damage increases with the increase of porosity. Through the curve analysis, the corresponding fitting formula is obtained, which accords with the exponential form.

The rock material is regarded as isotropic and release rate of damage strain energy under uniaxial stress state. The

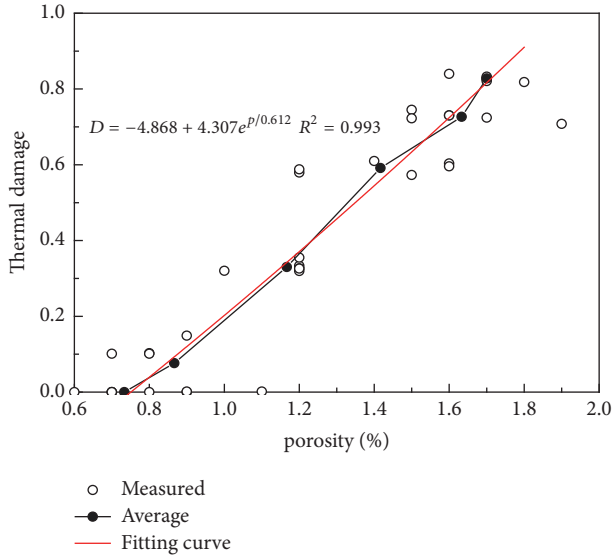

Figure 8: Relation of thermal damage and porosity.

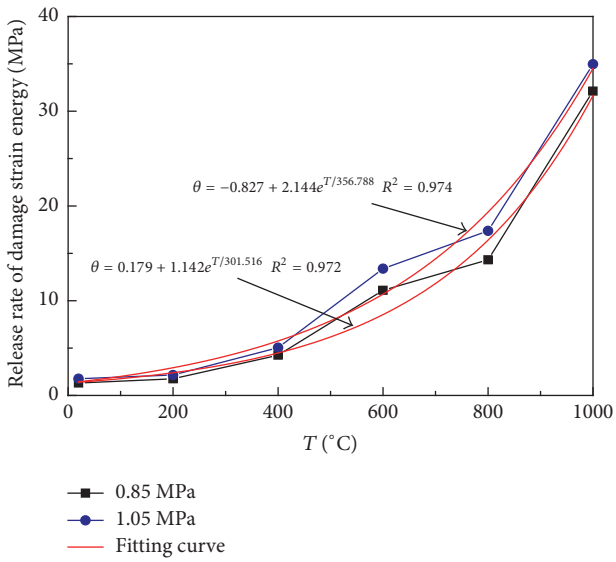

Figure 9: Relation of release rate of damage strain energy and temperature.

release rate of damage strain energy can better represent the damage and crack fracture and propagation inside rock. The relation between thermal damage and release rate of damage strain energy can be expressed as

$$\theta = \frac{\sigma^2}{2E(1-D)^2}, \tag{9}$$

where θ is release rate of damage strain energy, σ is peak stress, and E is elastic modulus, as shown in Figure 9.

As temperature rises, the release rate of damage strain energy of sandstone under the two types of impact pressure degrees shows a trend of gradually increasing in Figure 9. It is observed from the diagram that the release rate of damage strain energy has little changes from 20°C to 200°C. After 800°C, the release rate of damage strain energy increases rapidly. 200°C and 800°C are the threshold of damage strain energy release rate in the test. By regression analysis, release rate of damage strain energy and temperature meet the following equation:

0.85 MPa:

$$\theta = 0.179 + 1.142e^{T/301.516} \quad R^2 = 0.972. \tag{10}$$

1.05 MPa:

$$\theta = -0.827 + 2.144e^{T/356.788} \quad R^2 = 0.974. \tag{11}$$

3.5. Fracture of Sandstone. From the appearance changes of sandstone specimens as displayed in Figure 10, the failure of rock is obvious after high temperature treatment under the two impact pressure degrees. The sandstone is light gray at 200°C. What is more, above 400°C, sandstone samples start to gradually change from gray to light red. When the temperature reaches 800°C, although the surface integrity is still good, it is intuitively felt that the internal damage is widespread, which is due to the dehydration of minerals that undergo physical and chemical changes. With the increase of temperature, the main failure modes of the samples change: the size of the fragments decreases greatly and becomes more uniform; the number of powder particles increases; and there is an effect of temperature on the surface fracture.

3.6. Energy Evolution Curves. Analysis of energy transformation and conversion in the evolution of rock deformation and failure will contribute to reflecting the law of rock failure truly. Considering a rock unit of one unit volume, energy evolution equation of a rock unit in principle stress space can be expressed as (12) which took only the axial stress and strain into consideration [23]. The energy evolution curves of failure processes were fulfilled as shown in Figure 11.

$$\begin{aligned} U &= \int_0^{\varepsilon} \sigma \, d\varepsilon \\ U^e &= \frac{1}{2}\sigma\varepsilon^e \\ U^d &= U - U^e. \end{aligned} \tag{12}$$

where U is the total input strain energy of a rock unit generated by the external load and U^d and U^e stand, respectively, for the dissipated energy and the releasable elastic strain energy of a rock unit. The unit of U, U^d, and U^e is MJ/m^3, equivalent to the stress unit, MPa.

It is clear that the total input strain energy increases impact presses rate at the same temperature. The total input strain energy decreases with the temperature increasing when the impact pressure is the same. The whole process of energy evolution is divided into four stages: compression of fissures, linear deformation, yield of rock, and failure of rock. The change of elastic strain energy directly reflects the stability of rock during deformation and failure.

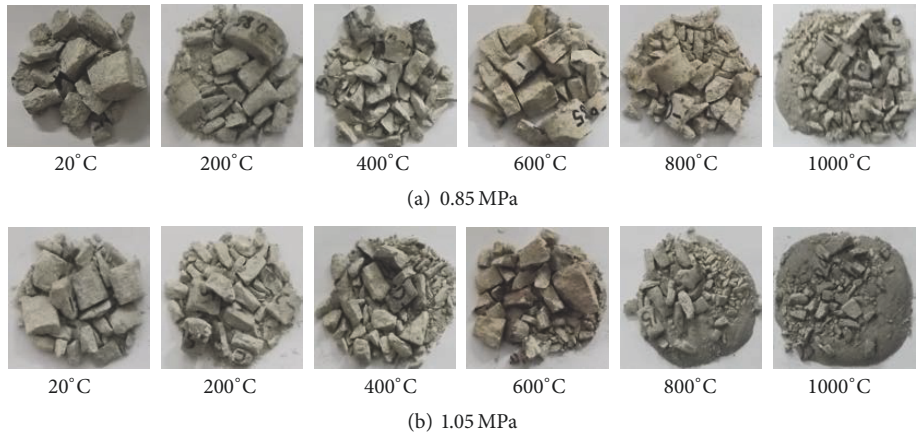

Figure 10: Dynamic compression fracture morphology of sandstone.

Taking into account the four stages of the energy evolution of sandstone during the dynamic characteristics, the energy dissipation ratio K and the formula are calculated as follows.

$$K_i = \frac{U_i^d}{U_i}, \tag{13}$$

where the subscript, i, fetches values from c, l, y, and f, representing the four stages, compression of fissures, linear deformation, yield of rock, and failure of rock.

Figure 12 shows $K_{c,l,y,f}$ of sandstone specimens after high temperature treatment. The energy dissipation ratio of the linear deformation and yield stage, $K_{1,y}$, is about from 0.50 to 0.75, the compression stage K_c is about 0.25, and the failure stage K_f is more than 1.25. K_f goes up a little as the temperature goes up. Actually, the distribution regularities of energy dissipation ratios of different stages are in good agreement with the energy evolution characteristics during the deformation and failure process of rock specimens, as presented previously.

The results show that no matter how the temperature changes, the energy dissipation of the sandstone will accord to a certain rule after high temperature treatment. There are differences in the failure stage of the sandstone. K_f of the sample has changed obviously after high temperature treatment. It can be seen from Figure 12 that the three stages of the sample before the peak points kept near a constant value, and K_f is minor increasing with the increase of temperature.

4. Discussion

In general, rock falls into the category of brittle material. The experimental results show that high temperature is the key factors that influence the physical and chemical mechanical properties of rock. The physical changes mainly include the loss of water in rock, the change of mass and volume, the initiation, and propagation of cracks, and the chemical changes mainly include the phase transition of crystal and the change of mineral composition.

The main reasons for these changes in the contents of the previous study are as follows.

Firstly, the different states of water (attached water, bound water, and mineral combined water) that exist inside the rock will evaporate after high temperature treatment. In particular, the weakly bound water can completely escape at about 150°C, and the strong bound water can completely escape only at the temperature of about 200°C to 300°C. When the temperature is above 400°C, especially at 450°C to 500°C, OH^- and H^- will be separated from the mineral skeleton and the mineral skeleton will be destroyed, which will destroy the mineral skeleton. A new mineral is formed. The crystalline water evaporates and escapes at less than 400°C. The loss of component water and crystalline water will lead to the destruction of the crystal structure of the mineral [21].

Secondly, because of the difference of thermal expansion coefficient of mineral composition in rock, there is thermal stress between crystal and fissure, which results in flaw and exfoliation of rock after high temperature treatment [12, 24].

Thirdly, After 400°C, the fissuring between the crystalline grains in the interior of rocks shows a cracking phenomenon and the crack can not be recovered. A variety of mineral related systems of sedimentary rocks change at high temperatures, the most significant of which is the reverse phase of quartz at 573°C from α to β phase. In addition, the clay minerals contained in the sandstone are kaolinite-dominant. The presence of minerals such as kaolinite by small weight loss intervals belongs to the dehydroxylation. The existence of clay minerals such as kaolinite may result in the loss of hydroxyl structural water. Therefore, the loss of hydroxyl structural water and from α to β transition of quartz also contributed to facture propagation [15–17].

5. Conclusions

The dynamic failure characteristics of sandstone after high temperature were studied by using a split Hopkinson pressure bar (SHPB) system. The physical and mechanical properties of sandstone treated at different temperatures were obtained. The damage characteristics, energy evolution, and failure mode of the specimen are analyzed. Based on the result, the following conclusions can be drawn.

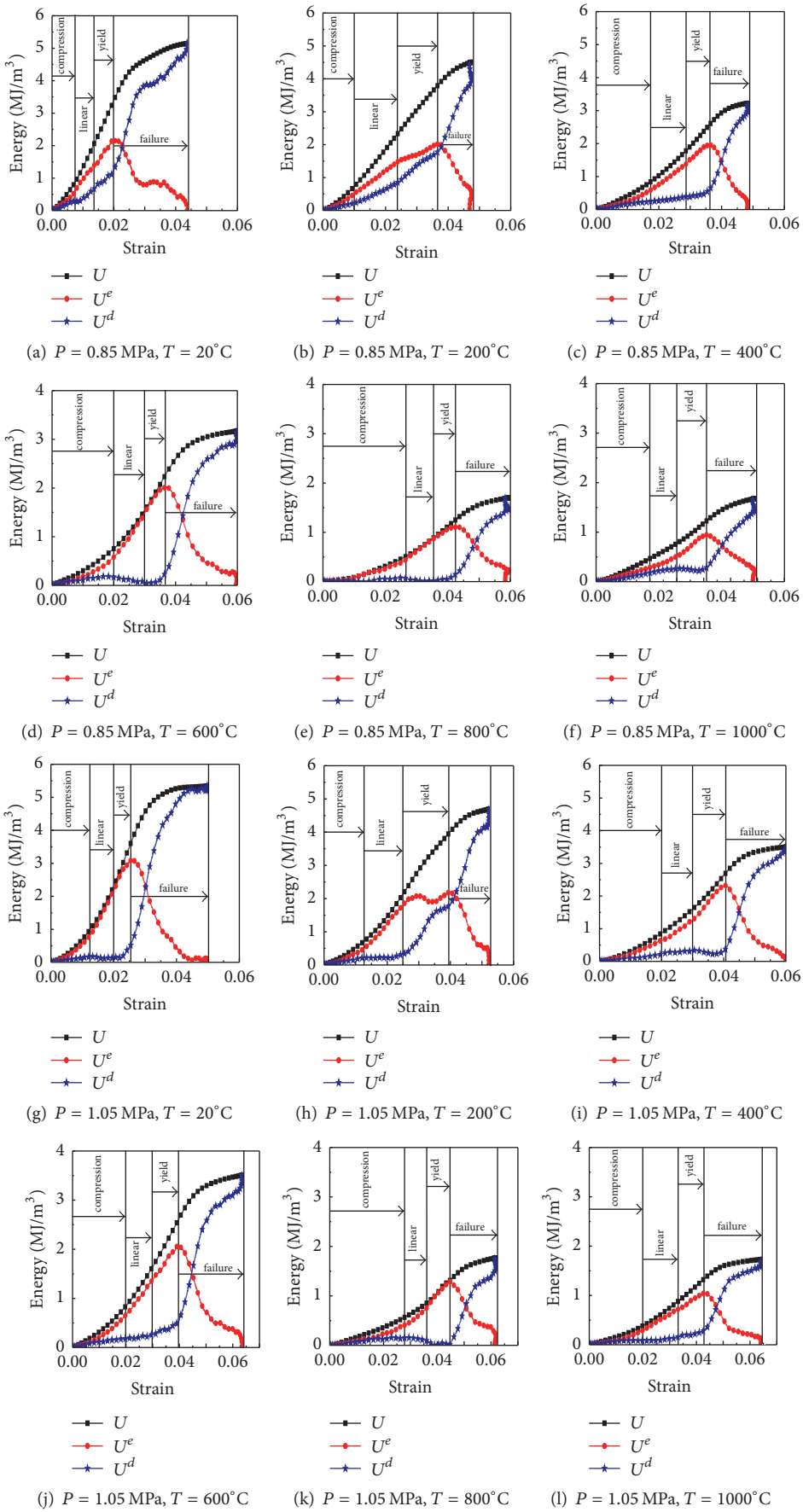

(a) $P = 0.85$ MPa, $T = 20^\circ$C (b) $P = 0.85$ MPa, $T = 200^\circ$C (c) $P = 0.85$ MPa, $T = 400^\circ$C

(d) $P = 0.85$ MPa, $T = 600^\circ$C (e) $P = 0.85$ MPa, $T = 800^\circ$C (f) $P = 0.85$ MPa, $T = 1000^\circ$C

(g) $P = 1.05$ MPa, $T = 20^\circ$C (h) $P = 1.05$ MPa, $T = 200^\circ$C (i) $P = 1.05$ MPa, $T = 400^\circ$C

(j) $P = 1.05$ MPa, $T = 600^\circ$C (k) $P = 1.05$ MPa, $T = 800^\circ$C (l) $P = 1.05$ MPa, $T = 1000^\circ$C

Figure 11: Energy evolution curves of sandstone after different temperature and impact pressure.

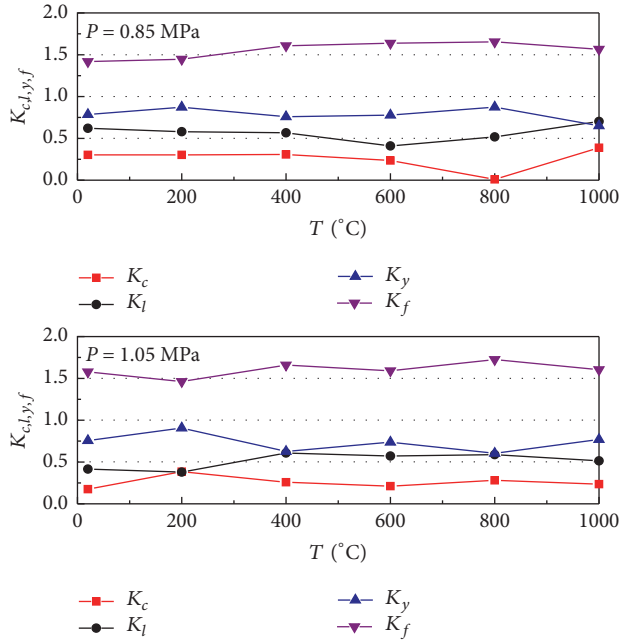

FIGURE 12: $K_{c,l,y,f}$ of sandstone specimens after high temperature treatment.

(1) In this paper, the peak stress and relative elastic modulus with temperature is studied. The peak stress and relative elastic modulus decrease with the increase of temperature, and the decreasing trend fits with the simple cubic equation, and the fitting degree is feasible. Above 600°C, dynamic peak stress and relative elastic modulus decrease rapidly.

(2) The thermal damage of rock is increasing with the increase of temperature, and the experimental results are in accordance with the logistic curve model. Thermal damage increases with the decrease of wave velocity and the increase of porosity. The release rate of damage strain energy can better represent the damage and crack fracture and propagation in rock. 200°C and 800°C are the threshold of damage strain energy release rate.

(3) The change of energy can better reflect the rock breakage. The total input strain energy decreases with the temperature increasing when the impact pressure is the same. Its total input strain energy decreases with the increase of processing temperature and decreases sharply when the temperature is over 600°C. The variation of total input energy has small change at the range from 400°C to 600°C. The three stages of the sample before the peak points kept near a constant value, and K_f is little increasing with the increase of temperature.

Conflicts of Interest

The authors declare no conflicts of interest.

Acknowledgments

The work is financially supported by the National Natural Science Foundation of China (51774011).

References

[1] D. P. Adhikary and H. Guo, "Modelling of Longwall Mining-Induced Strata Permeability Change," *Rock Mechanics and Rock Engineering*, vol. 48, no. 1, pp. 345–359, 2014.

[2] H. Xie, Y. Ju, F. Gao, M. Gao, and R. Zhang, "Groundbreaking theoretical and technical conceptualization of fluidized mining of deep underground solid mineral resources," *Tunnelling and Underground Space Technology*, vol. 67, pp. 68–70, 2017.

[3] A. P. Sasmito, J. C. Kurnia, E. Birgersson, and A. S. Mujumdar, "Computational evaluation of thermal management strategies in an underground mine," *Applied Thermal Engineering*, vol. 90, 2017.

[4] Z. Yang, "Key Technology Research on the Efficient Exploitation and Comprehensive Utilization of Resources in the Deep Jinchuan Nickel Deposit," *Engineering Journal*, vol. 3, no. 4, pp. 559–566, 2017.

[5] E. Shoko, B. McLellan, A. L. Dicks, and J. C. D. da Costa, "Hydrogen from coal: Production and utilisation technologies," *International Journal of Coal Geology*, vol. 65, no. 3-4, pp. 213–222, 2006.

[6] Z. X. Zhang, J. Yu, S. Q. Kou, and P.-A. Lindqvist, "Effects of high temperatures on dynamic rock fracture," *International Journal of Rock Mechanics and Mining Sciences*, vol. 38, no. 2, pp. 211–225, 2001.

[7] S. Liu and J. Y. Xu, "Study on dynamic characteristics of marble under impact loading and high temperature," *International Journal of Rock Mechanics and Mining Sciences*, vol. 62, pp. 51–58, 2013.

[8] S. Liu and J. Xu, "An experimental study on the physico-mechanical properties of two post-high-temperature rocks," *Engineering Geology*, vol. 185, pp. 63–70, 2015.

[9] T.-B. Yin, R.-H. Shu, X.-B. Li, P. Wang, and X.-L. Liu, "Comparison of mechanical properties in high temperature and thermal treatment granite," *Transactions of Nonferrous Metals Society of China*, vol. 26, no. 7, pp. 1926–1937, 2016.

[10] T.-B. Yin, K. Peng, L. Wang, P. Wang, X.-Y. Yin, and Y.-L. Zhang, "Study on Impact Damage and Energy Dissipation of Coal Rock Exposed to High Temperatures," *Shock and Vibration*, vol. 2016, Article ID 5121932, 2016.

[11] B. Kong, Z. Li, and E. Wang, "Fine characterization rock thermal damage by acoustic emission technique," *Journal of Geophysics and Engineering*, vol. 15, no. 1, pp. 1–12, 2018.

[12] J. Zhou, J. Wei, T. Yang, W. Zhu, L. Li, and P. Zhang, "Damage analysis of rock mass coupling joints, water and microseismicity," *Tunnelling and Underground Space Technology*, vol. 71, pp. 366–381, 2018.

[13] X. Li and D. Gu, "Energy dissipation of rock under impulsive loading with different waveforms," *Combustion, Explosion, and Shock Waves*, vol. 14, no. 2, pp. 129–139, 1994.

[14] J. Jin, P. Cao, Y. Chen, C. Pu, D. Mao, and X. Fan, "Influence of single flaw on the failure process and energy mechanics of rock-like material," *Computers & Geosciences*, vol. 86, pp. 150–162, 2017.

[15] Q. Sun, C. Lü, L. Cao, W. Li, J. Geng, and W. Zhang, "Thermal properties of sandstone after treatment at high temperature,"

International Journal of Rock Mechanics and Mining Sciences, vol. 85, pp. 60–66, 2016.

[16] X. Liu, S. Yuan, Y. Sieffert, S. Fityus, and O. Buzzi, "Changes in Mineralogy, Microstructure, Compressive Strength and Intrinsic Permeability of Two Sedimentary Rocks Subjected to High-Temperature Heating," *Rock Mechanics and Rock Engineering*, vol. 49, no. 8, pp. 2985–2998, 2016.

[17] Q.-L. Ding, F. Ju, X.-B. Mao, D. Ma, B.-Y. Yu, and S.-B. Song, "Experimental investigation of the mechanical behavior in unloading conditions of sandstone after high-temperature treatment," *Rock Mechanics and Rock Engineering*, vol. 49, no. 7, pp. 2641–2653, 2016.

[18] ISRM, "The complete ISRM suggested methods for rock characterization, testing and monitoring: 1974–2006," in *Suggested methods prepared by the commission on testing methods, International Society for Rock Mechanics*, Ulusay and Hudson, Eds., p. 628, ISRM Turkish National Group, Ankara, Turkey, 2007.

[19] X. Chen and Z. Xu, "The ultrasonic P-wave velocity-stress relationship of rocks and its application," *Bulletin of Engineering Geology and the Environment*, vol. 76, no. 2, pp. 661–669, 2017.

[20] K. Karaman, A. Kaya, and A. Kesimal, "Effect of the specimen length on ultrasonic P-wave velocity in some volcanic rocks and limestones," *Journal of African Earth Sciences*, vol. 112, pp. 142–149, 2015.

[21] W. Zhang, Q. Sun, S. Hao, J. Geng, and C. Lv, "Experimental study on the variation of physical and mechanical properties of rock after high temperature treatment," *Applied Thermal Engineering*, vol. 98, pp. 1297–1304, 2016.

[22] X. Li and G. Yin, "Logistic models with regime switching: permanence and ergodicity," *Journal of Mathematical Analysis and Applications*, vol. 441, no. 2, pp. 593–611, 2016.

[23] R. Solecki and R. J. Conant, *Advanced Mechanics of Materials*, Oxford University Press, London, UK, 2003.

[24] B. Kong, E. Wang, Z. Li et al., "Electromagnetic radiation characteristics and mechanical properties of deformed and fractured sandstone after high temperature treatment," *Engineering Geology*, vol. 209, pp. 82–92, 2016.